Article

On the Role of Poly-Glutamic Acid in the Early Stages of Iron(III) (Oxy)(hydr)oxide Formation

Miodrag J. Lukić [1,2,*], Felix Lücke [1], Teodora Ilić [3,4], Katharina Petrović [1] and Denis Gebauer [1,*]

1. Institute of Inorganic Chemistry, Leibniz University Hannover, 30167 Hannover, Germany; luecke@acc.uni-hannover.de (F.L.); katharina.petrovic@aci.uni-hannover.de (K.P.)
2. Institute of Technical Science of SASA, 11000 Belgrade, Serbia
3. Faculty of Physical Chemistry, University of Belgrade, 11000 Belgrade, Serbia; teodora@ugr.es
4. Faculty of Sciences, Department of Mineralogy and Petrology, University of Granada, 18071 Granada, Spain
* Correspondence: lukic@acc.uni-hannover.de (M.J.L.); gebauer@acc.uni-hannover.de (D.G.)

Abstract: Nucleation of minerals in the presence of additives is critical for achieving control over the formation of solids in biomineralization processes or during syntheses of advanced hybrid materials. Herein, we investigated the early stages of Fe(III) (oxy)(hydr)oxide formation with/without polyglutamic acid (pGlu) at low driving force for phase separation (pH 2.0 to 3.0). We employed an advanced pH-constant titration assay, X-ray diffraction, thermal analysis with mass spectrometry, Fourier Transform infrared spectroscopy, and scanning electron microscopy. Three stages were observed: initial binding, stabilization of Fe(III) pre-nucleation clusters (PNCs), and phase separation, yielding Fe(III) (oxy)(hydr)oxide. The data suggest that organic–inorganic interactions occurred via binding of olation Fe(III) PNC species. Fourier Transform Infrared Spectroscopy (FTIR) analyses revealed a plausible interaction motif and a conformational adaptation of the polypeptide. The stabilization of the aqueous Fe(III) system against nucleation by pGlu contrasts with the previously reported influence of poly-aspartic acid (pAsp). While this is difficult to explain based on classical nucleation theory, alternative notions such as the so-called PNC pathway provide a possible rationale. Developing a nucleation theory that successfully explains and predicts distinct influences for chemically similar additives like pAsp and pGlu is the Holy Grail toward advancing the knowledge of nucleation, early growth, and structure formation.

Keywords: pre-nucleation clusters; iron (III) hydrolysis; poly-L-glutamic acid; nucleation; additive-controlled mineralization

1. Introduction

Nucleation of inorganic minerals in the presence of (bio)macromolecules increasingly attracts research attention owing to the possibility of progression toward controlling the synthesis of advanced materials and the understanding of biomineralization processes. Iron (oxy)(hydr)oxides are important (bio)-minerals [1], and their nucleation and crystal growth are closely related to the presence of bio-macromolecules in natural systems [2–4]. There are multiple roles that additives can play, while it has already been well established that nucleation in the presence of some additives, especially in the early stages of mineralization, cannot be satisfactorily explained from the viewpoint of classical nucleation theory [5].

The literature data on iron (oxy)(hydr)oxide nucleation is vast, and the formation of akagenéite, ferrihydrite, maghemite, and hematite has been extensively studied [6,7]. Recently, magnetite crystallization has been described as a colloidal assembly process [8], while the formation of hematite mesocrystals was proposed to proceed via interface-driven nucleation and assembly [9]. The influence of sodium oxalate on the formation of hematite mesocrystals was explained by a change in solution chemistry in the interfacial region of the solid [9]. However, it is also important to study the changes that occur in the early, that is, the prenucleation stage, in a homogeneous solution, where Fe(III) prenucleation cluster

(PNC) species and organic additives interact and may lead to the formation of distinct solids. Different additives exhibit multiple effects on the nucleation process of different minerals, whereas the same additive can even promote and retard nucleation depending on the specific mineral [10]. Scheck et al. showed that the presence of polyaspartic acid facilitates the nucleation in the Fe(III) system by promoting the olation–oxolation transition and thereby decreasing the dynamics of olation PNCs, which is the main event underlying initial phase separation according to the non-classical PNC pathway. This allows understanding of the nucleation mechanism in this inorganic–organic hybrid system [11]. Furthermore, olated PNCs are fundamental species toward hematite formation from acidic solutions at low driving force for phase separation and elevated temperatures via an entropically-driven process, avoiding a high-temperature treatment or the hydrothermal processing necessary to transform akagenéite or ferrihydrite phases, that usually precipitate initially, into hematite [12].

Given that poly-aspartic acid strongly inhibits calcium carbonate but promotes iron(III)(oxy)(hydr)oxide formation [11,13], while poly-glutamic acid (pGlu) exhibits only a weak influence on calcium mineral formation [13], exploring the influence of pGlu on the early stages of mineralization in the Fe(III) system seems promising. Poly-glutamic acid (pGlu) is an important biopolymer, extensively used in food, medical, and wastewater applications [14]. Its addition to inorganic minerals can improve the overall (bio)-response, as in recently formulated alum-pGlu vaccine adjuvants [15], sorbent materials [16], and contrast agents [17]. Besides, pGlu serves as a model molecule to study the interaction of inorganic systems with polypeptides, assessing preferential binding sites and conformational changes [18], since it exists in biomolecular templates for heterogeneous nucleation and growth of iron(oxy)(hydr)oxide nanoparticles [19].

Herein, we investigate for the first time the effect of pGlu acid sodium salt with two different degress of polymerization (20/50) on the nucleation of iron(III) (oxy)(hydr)oxide at low driving force for phase separation and ambient temperature. We employed an advanced titration assay and several physicochemical methods (X-ray diffraction (XRD), Fourier transform infrared spectrometry (FTIR), thermogravimetry/differential thermal analysis (TG/DTA), differential scanning calorimetry-mass spectrometry (DSC-MS), scanning electron microscopy (SEM)) to characterize samples isolated from the titrations. Moreover, we explore the effect of the additive concentration on the early stages of Fe(III) mineralization. Compared to polyaspartic acid, pGlu shows a distinct behavior in three different stages during Fe(III) hydrolysis. The pGlu sodium salts investigated in this study did not induce sudden nucleation of Fe (oxy)(hydr)oxide, as opposed to polyaspartic acid in prior work [11]. Rather, pGlu suppresses Fe(III) hydrolysis, and it is incorporated in the resulting hybrid material (15 wt.%), and seems to yield akagenéite with higher crystallinity than in the reference experiments without additives.

2. Materials and Methods

Fe(III) nucleation was studied in the presence of sodium salts of the alpha form (please see Scheme 1) of poly-L-glutamic (pGlu) acid, with 20 (pGlu20, Mw = 2500 g/mol) and 50 (pGlu50, Mr = 7500 g/mol) monomeric units. Commercial polymers with narrow molecular weight distribution and a defined number of monomeric units were used: pGlu20 (NanoSoft Polymers, Winston-Salem, NC, USA) and pGlu50 (Alamanda Polymers, Huntsville, AL, USA). We have applied a pH-constant titration assay (Methrom, Titrando 905, Herisau, Switzerland) at low driving force for phase separation to induce Fe(III) hydrolysis and nucleation. The experiments were performed with and without the additives at different pH values, namely, 2.0, 2.5, and 3.0. A solution of 0.1 M Fe(III) (Sigma, Fe(III)Cl$_3$·6H$_2$O) in 0.1 M HCl (Merck, standard solution) was dosed at a dosing rate of 10 μL/min into polymer solutions. The polymer solutions were prepared by dissolving a solid polymer in an HCl solution with a pre-adjusted pH value. Any deviation in the pH value of the solutions after the polymer addition was compensated by the addition of 0.1 M HCl and 0.05 M NaOH. The reaction volume was 35 ± 2 mL. Titration curves are shown

as $c_{ex}(OH^-)$ vs. $c_{added}(Fe^{3+})$, where the former quantity represents the concentration of base added in excess to keep the pH value constant, and the latter value represents the concentration of Fe(III) in the solution upon continuous dosing. The base was added to compensate for the release of H^+ ions due to Fe(III) hydrolysis and binding to the additive, so that $c_{ex}(OH^-)$ is equal to $c_{released}(H^+)$ used in the further analysis. The thermal analysis of pGlu20 was performed coupled with mass spectrometry analysis in an Ar-20%O_2 atmosphere to determine the characteristic temperatures at which chemical processes produce species in the gas phase (STA 409 PC Luxx®, NETZSCH, Selb, Germany). Thermal analysis (TG/DTA) of pure Fe and Fe-polymer composite powders drawn after titrations was performed in synthetic air without mass spectrometry (STA 429, NETZSCH, Selb, Germany). All measurements were performed at a heating rate of 5 K/min, up to 1000 °C. X-ray diffraction (XRD, Stoe StadIP, with a MYTHEN detector, Darmstadt, Germany) was used to determine the phase composition of the powders drawn after titrations at pH 3.0 with and without the additive and of the same materials after the thermal analysis up to 1000 °C. The device used Cu-Kα radiation and operated at 40 kV and 30 mA. The samples were recorded in a *2θ* range from 5 to 90°, with a step size of 0.1° *2θ* and a dwell time of 15 s per step. The presence of the characteristic functional groups was assessed by attenuated total reflection Fourier-Transform IR spectrometry, ATR-IR (Bruker Tensor 27, Bruker, Billerica, MA, USA), by direct depositing of powders on the ATR crystal. The measurements were performed in the range from 800 to 4000 cm^{-1}, with a resolution of 1 cm^{-1} and 64 scans. All spectra were baseline-corrected. The morphology of the gold-coated precipitated powder was characterized using scanning electron microscopy (SEM, JEOL-AJ5 JSM 6610, Tokyo, Japan) and a field-emission SEM device (FE-SEM, JEOL JSM-6700F, Tokyo, Japan). The powders were ground before gold-coating. The polymers were used as received, without further purification.
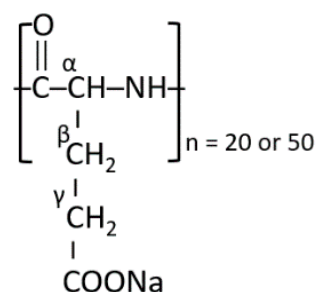

Scheme 1. Chemical structure of the used sodium salt of poly-L-glutamic acid.

3. Results

The titration curves obtained for the iron solutions without additive serve as a reference, and are consistent with previously published results [20]. Without additive, there is very little Fe(III) hydrolysis at pH 2.0, while it extensively occurs at pH 2.5 and 3.0, Figure 1a. The initial linear region of the titration curves of the Fe(III) system at pH 2.5 and 3.0 corresponds to the prenucleation stage, where iron mainly exists in the form of olation Fe(OH)$_2{}^+$ PNCs [20]. The base consumption starts to increase and deviate from the linear regime with further Fe(III) addition, indicating nucleation onset via an irreversible olation-oxolation transition [20]. The extent of hydrolysis is also expressed as the $c_{released}(H^+)/c_{added}(Fe^{3+})$ ratio vs. $c_{added}(Fe^{3+})$, Figure 1b, providing an alternative insight into the hydrolysis extent with ongoing iron addition. The quantity $c_{released}(H^+)/c_{added}(Fe^{3+})$ is a unitless quantity giving the ratio of produced protons per hexa-aqua iron(III) added, at any time during the titrations. Thus, it reflects the changes in chemical equilibrium upon Fe(III) dosing. In the Fe(III) system without additive, the released H^+ ions originate only from Fe(III) hydrolysis, while in the system with additive, they originate from both Fe(III) hydrolysis and binding to the additive (i.e., due to releasing protons from the carboxylic acid functions of the polymer). It is apparent that the $c_{released}(H^+)/c_{added}(Fe^{3+})$ value increases with pH, and

at pH 3.0, the system undergoes extensive hydrolysis at very low Fe(III) concentrations, exhibiting the nucleation onset already below ~0.4 mM Fe(III).
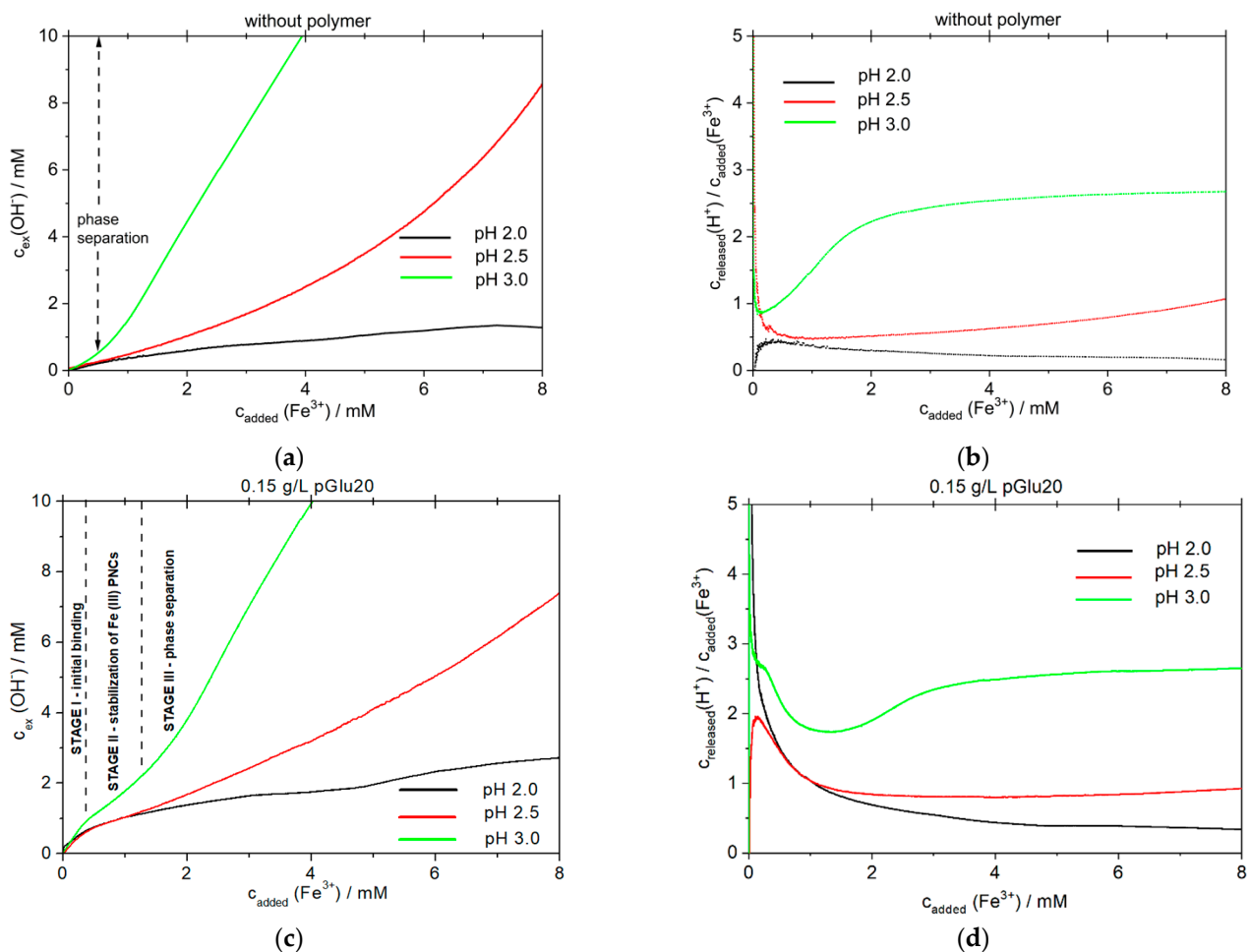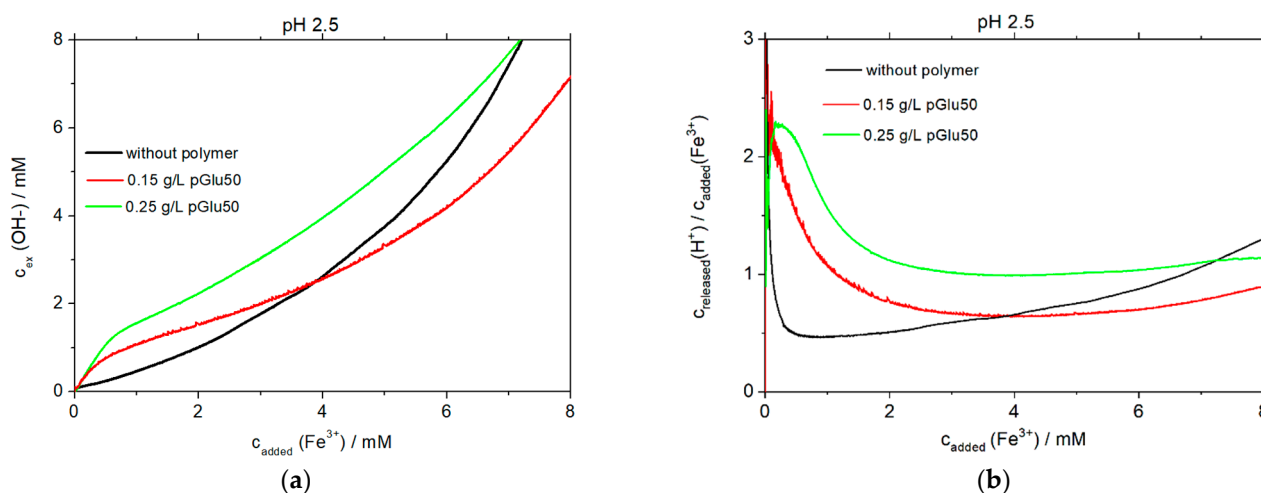

Figure 1. Titration curves of the Fe(III) system: (**a**) without polymer and (**b**) the corresponding $c_{released}(H^+)/c_{added}(Fe^{3+})$ ratio vs. $c_{added}(Fe^{3+})$ curves; (**c**) 0.15 g/L pGlu20 and (**d**) the corresponding $c_{released}(H^+)/c_{added}(Fe^{3+})$ ratio vs. $c_{added}(Fe^{3+})$ curves.

On the other hand, in the presence of pGlu20, at all the investigated pH values, the system exhibits a very distinct behavior. All titration curves show a strong initial increase in the base consumption, Figure 1c, implying a strong release of H^+. After the initial stage, the titration curves enter a steady-state region, with a stable increase in the base consumption rate. The slope of the titration curve at pH 2.0 in the presence of pGlu20 does not change significantly with further Fe(III) addition, confirming a low hydrolysis rate. At pH 2.5 and 3.0, the system leaves the second stable hydrolysis regime with ongoing Fe(III) addition, entering the third stage with an increased base consumption, similar to the Fe(III) behavior without the additive. At pH 2.5 and 3.0, the second characteristic stage in the titration curve in the presence of pGlu20 has a lower slope than that of the titration curves without the polymer for the same Fe(III) concentration, indicating suppressed Fe(III) hydrolysis after the initial interaction of Fe(III) PNCs with the organic component. This is better illustrated in the $c_{released}(H^+)/c_{added}(Fe^{3+})$ ratio vs. $c_{added}(Fe^{3+})$ curves, Figure 1d. The initial $c_{released}(H^+)/c_{added}(Fe^{3+})$ values are high for all the pH values. At pH 2.5, the $c_{released}(H^+)/c_{added}(Fe^{3+})$ ratio without the additive continuously increases from (Fe^{3+}) ~2 mM. In comparison, the ratio remains stable up to ~5 mM, implying that the presence of pGlu20 stabilizes the hydrolyzed Fe(III) species. At pH 3.0, the effect of the presence of pGlu20 is very apparent, showing a wide concentration range of Fe(III), in which the extensive hydrolysis is suppressed although Fe(III) ions are continuously dosed into the

solution. Extensive hydrolysis is effectively suppressed up to 1.8 mM of added Fe(III), which is distinct from the behavior without the additive, where the phase separation occurs at very low Fe(III) concentrations. The $c_{released}(H^+)/c_{added}(Fe^{3+})$ ratio in the second stage at pH 3.0 exhibits apparent stagnation in the hydrolysis–condensation–phase separation event, potentially because the additive effectively binds Fe(III) PNC species formed in the solution. The titration curve regains the shape characteristic for the intensive hydrolysis, implying that the Fe(III) hydrolysis and nucleation proceed at this point despite the presence of the additive.

Besides the chemical composition and structure, polyelectrolytes may exhibit different effects on the early stages of mineralization depending on the length of the main chain. Thus, we performed the titration experiments in the presence of pGlu with 50 monomeric units (pGlu50, Mw 7500 g/mol) at pH 2.5, Figure 2. The effect of polymer concentration, i.e., 0.15 and 0.25 g/L, was also assessed. Similar to pGlu20, the interaction with the additive is distinct. The presence of the same concentration of pGlu50 (0.15 g/L) influences the hydrolysis behavior in a similar manner as pGlu20, Figure 2a. The increase in the pGlu50 concentration to 0.25 g/L shifts the length of the initial hydrolysis step toward higher Fe(III) concentrations, confirming that the first jump correlates with the absolute amount of the additive, while the curves retain qualitatively the same shape. This is also apparent in the $c_{released}(H^+)/c_{added}(Fe^{3+})$ratio vs. $c_{added}(Fe^{3+})$ curves, indicating the stabilization of the Fe(III) PNC species by pGlu50, where the rate of H^+ release is suppressed in the presence of the additive.

Figure 2. (**a**) Titration curves at pH 2.5 without the polymer and in the presence of pGlu50 at 0.15 and 0.25 g/L; (**b**) the corresponding $c_{released}(H^+)/c_{added}(Fe^{3+})$ ratio vs. $c_{added}(Fe^{3+})$ curves.

Figure 3a shows the XRD diffractorgrams of the solids isolated from the Fe(III) system without additives and in the presence of 0.15 g/L pGlu20 after titrations at pH 3.0 and upon the thermal treatment up to 1000 °C (after the TG/DTA analysis). After the titrations, the akagenéite (β-FeOOH) phase [21] is formed with and without pGlu20. This phase is characteristic for the precipitation of Fe(III)(oxy)(hydr)oxide from chloride solutions, and contains chloride ions in its structure. However, the reflections of the sample with pGlu20 are better defined than those obtained without the polymer, suggesting a higher crystallinity of the material synthesized in the presence of the additive. After the thermal treatment, both the systems are transformed in the hematite phase [22], showing no apparent differences in the XRD patterns. Figure 3b shows FTIR spectra of pure pGlu20 and of the powders drawn at pH 3.0 without additive and pH 2.5 in the presence of 0.15 g/L pGlu20 (upper panel) with the amide region separately shown to better assess any spectral changes (lower panel). The FTIR spectrum of pGlu20 exhibits a band of medium-intensity in the region of the amide I vibration at 1645 cm^{-1}, a very strong complex band consisting of two peaks with maxima at 1561 and a 1519 cm^{-1} in the amide II region,

and another strong peak at 1394 cm^{-1}, with a low-intensity shoulder at 1444 cm^{-1}. The hydrogen-bonded N-H stretching vibration of pGlu20 appears around 3248 cm^{-1}, while this area can also be ascribed to the hydroxyl group stretching vibration around 3300 cm^{-1}. According to the study of Nickels et al., deuterated poly-L-glutamic acid with a random coil secondary structure shows bands at 1561 and 1646 cm^{-1} [23], so it is assumed that the soluble pGlu20 sodium salt used in this study adopts the random coil structure. The peak at 1645 cm^{-1} is characteristic for the amide I vibration, between 1600 and 1700 cm^{-1}, mainly due to the C=O stretching vibration and a specific contribution from the C-N band. The region between 1500 and 1600 cm^{-1} is characteristic for amide II vibrations, consisting of a dominant contribution of N-H bending and C-N stretching vibrations. The sample drawn after titration at pH 2.5 in the presence of 0.15 g/L pGlu20 shows vibrational bands characteristic for pGlu20, mostly implying the preserved structure of the additive upon the interaction with Fe(III) species. However, the amide region of the polypeptide shows some shifts of the characteristic bands, implying conformational changes. In the amide II region, the most intense broad band with maxima at 1561 and a 1519 cm^{-1} turns into a single band at 1530 cm^{-1}, implying conformational changes, probably due to a change in hydrogen bonding of the polypeptide chain [24]. The band at 1394 cm^{-1} due to the -COO$^-$ symmetric stretching vibration [25] exhibits a blue-shift to 1405 cm^{-1}, suggesting the primary interaction point between hydrolyzed Fe(OH$^-$)$^{2+}$ PNC species and the polymer. On the other hand, the amide I N-H vibration at 1645 cm^{-1} of the pGlu20 sodium salt [26] is slightly red-shifted to 1640 cm^{-1}.
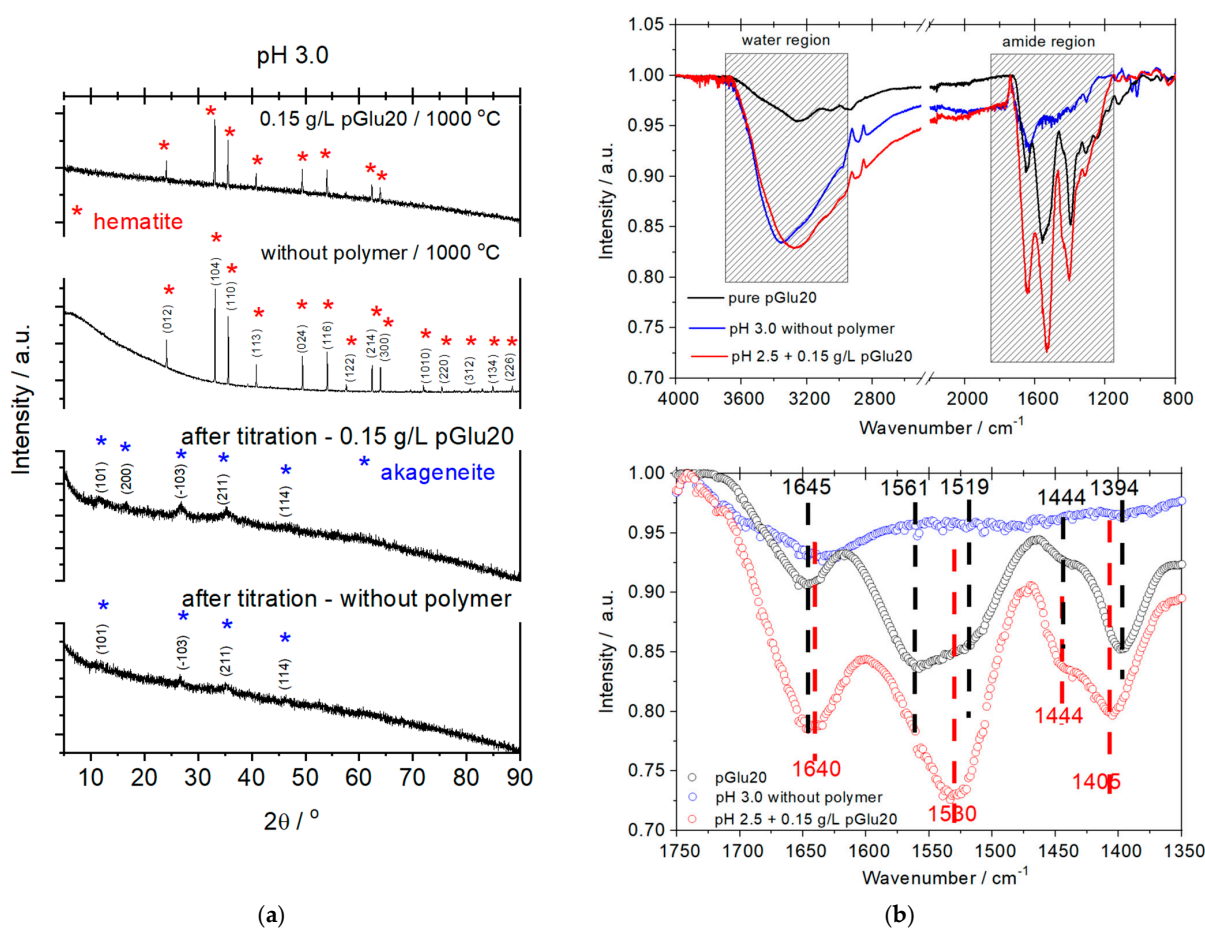

Figure 3. (**a**) XRD patterns of powders drawn after titrations at pH 3.0 and after the non-isothermal TG/DTA analysis up to 1000 °C. (**b**) FTIR spectra of the as-received pGlu20 powder and the reference Fe(III)-oxyhydroxide after titrations at pH 3 and the Fe(III) + 0.15 g/L pGlu20 sample after titration at pH 2.5 (**upper** panel) with a magnified amide region (**lower** panel).

We have further analyzed the characteristics of the materials isolated from the titration experiments. Figure 4a shows TG/DTA curves of the materials drawn at pH 3.0 without the additive and in the presence of 0.15 g/L pGlu20. The reference Fe(III) system exhibits a mass decrease at ~100 °C, originating from the release of physically adsorbed water. The weight loss monotonously proceeds up to 750 °C, implying the loss of some structural water during the thermal crystallization of the material. Afterward, the material is thermally stable, exhibiting the total mass loss of 10.2%. In the case of the solid obtained with 0.15 g/L pGlu20, the system behaves completely differently. The first mass drop of ~10% corresponds to the loss of loosely bound water molecules around 100 °C. The second weight-loss step of ~8% appears at ~258 °C, accompanied by a small exothermic feature in the DTA curve, which implies the onset of the degradation of the organic phase. Furthermore, the DTA curve exhibits a very sharp and intensive peak at 357 °C accompanied by a 2% weight loss, which implies a structural rearrangement in the material. Above 500 °C occurs the final mass loss step, indicating the polymer combustion. The analysis of the thermal behavior of pure pGlu20 was conducted using a coupled TG/dTG-MS analysis in Ar-20%O_2 atmosphere, Figure 4b. The release of H_2O (m/z = 18) occurs at ~100 °C, while H_2O and CO_2 (m/z = 44) also appear in the temperature range from 300 to 370 °C, indicating the onset of the polymer chemical bond degradation. The complete polymer combustion happens at 630 °C. Comparing the thermal behavior of the pure pGlu20 and the inorganic solid with 0.15 g/L pGlu20, the organic component in the composite FeOx-pGlu exhibits a slightly worse thermal stability.
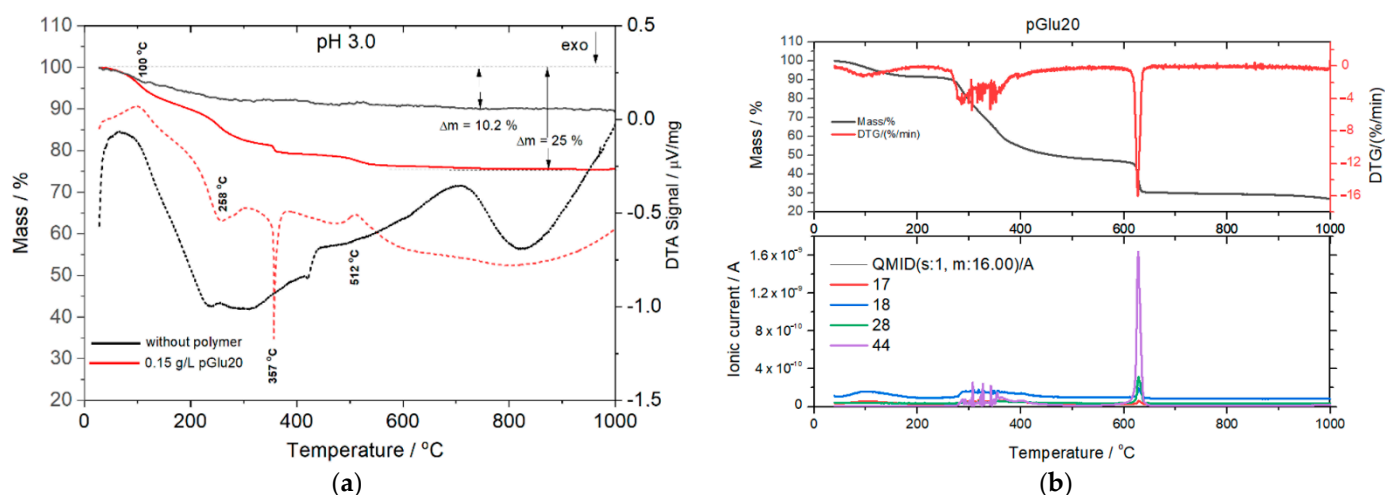
Figure 4. (**a**) TG/DTA curves of the materials drawn at pH 3.0 without the additive and in the presence of 0.15 g/L pGlu20 measured at 5 K/min up to 1000 °C in an air atmosphere. (**b**) TG/dTG-MS curves of pGlu20 powder at 5 K/min up to 1000 °C in an Ar-20%O_2 atmosphere.

SEM micrographs in Figure 5 show powders isolated from titrations under different conditions. Without pGlu, akagenéite powders at pH 2.5 and 3.0 exhibit spherical particles with a berry-like morphology and a high degree of particle aggregation. In the presence of 0.15 g/L pGlu20 at pH 3.0, the spherical morphology of the particles is degraded, and particles are agglomerated into bigger species. Furthermore, some of these agglomerates exhibit a characteristic polyhedral crystal shape, indicating a distinct crystal growth pathway and higher crystallinity, which is also suggested by the XRD patterns shown in Figure 4a. In the presence of 0.15 g/L of pGlu50 at pH 2.5, larger polyhedral agglomerates are apparent, and the remaining primary particles have an irregular shape.
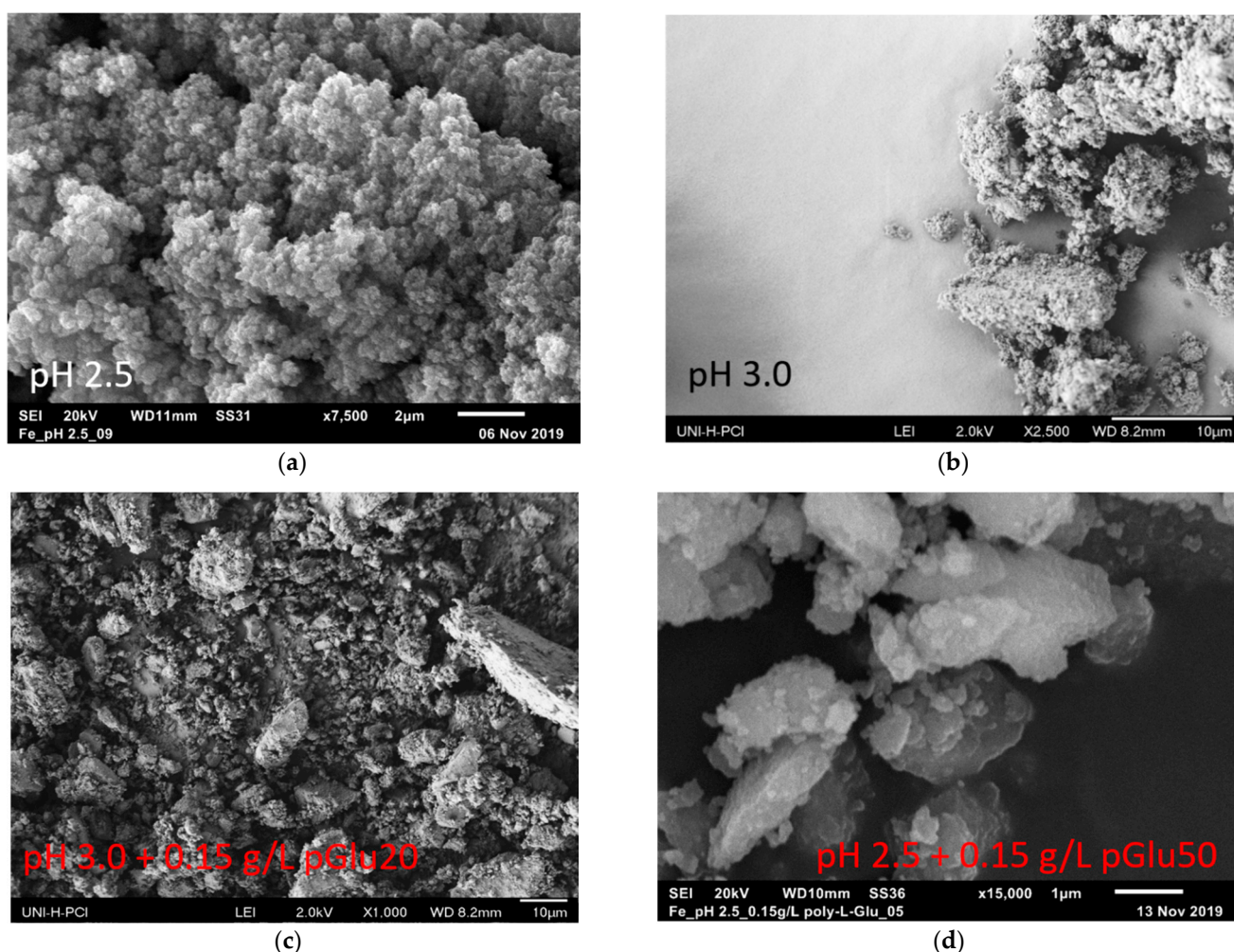
Figure 5. SEM micrographs of powders drawn after titrations: (**a**) pH 2.5 and (**b**) pH 3.0 without an additive; (**c**) pH 3.0 + 0.15 g/L pGlu20, and (**d**) pH 2.5 + 0.15 g/L pGlu50.

4. Discussion

We systematically investigated for the first time the early stages of Fe(III) (oxy)(hydr)oxide formation at pH values of 2.0, 2.5, and 3.0 in the presence of pGlu sodium salt with two different polypeptide lengths (20 (pGlu20) and 50 (pGlu50) monomer units) and molecular weights (2500 and 7500 g/mol, respectively), also assessing the effect of concentration in the case of pGlu50. For that purpose, we applied a very slow dosing of 0.1 M Fe(III) solution in 0.1 M HCl and kept the pH value constant by counter-titration with freshly-prepared 0.05 M NaOH solution. Our experimental titration data indicate the apparent interaction between Fe(III) olation PNCs and both pGlu 20 and pGlu50 additives. Three stages in the titration curves can be clearly distinguished. It is reasonable to assume that the initial interaction of Fe(III) PNC species in the prenucleation regime occurs at the available side-chain COOH groups of the additive. This is accompanied by an increase in the base consumption to keep the pH constant due to the H^+ release from the polymer. It is interesting to assess the deflection points between the first and the second stage in the titration curves quantitatively. Namely, for pGlu20, at an additive concentration of 0.15 g/L, independent of the pH value, this transition occurs for the concentration of added Fe(III) of 0.28–0.30 mM, which corresponds to the prenucleation regime in the Fe(III) system. This yields an $n(COOH):n(Fe^{3+})_{added}$ mole ratio of ~4:1, according to the initial amount of additive and the amount of moles of Fe(III) present in the system. For the same additive concentration (0.15 g/L) and pH 2.5, the system exhibits a similar behavior in the case of pGlu50, where the transition happens at a concentration of added Fe(III) of

0.24 mM, which again corresponds to an $n(COOH):n(Fe^{3+})_{added}$ mole ratio of ~4:1 due to a higher molecular weight of the additive. When the pGlu50 concentration is 0.25 g/L, the characteristic deflection point between the two hydrolysis stages occurs at 0.41 mM of added Fe(III), corresponding to the same $n(COOH):n(Fe^{3+})_{added}$ mole ratio of ~4:1. This ratio does not correspond to the simple binding of monomeric Fe(III) species to carboxyl groups but rather implies that Fe(III) species are present as highly dynamic olation PNC clusters, which have been detected in earlier work [20], that effectively interact with the additive as a whole. In the case of electrostatic binding of monomeric Fe(III) species, a maximum $n(COOH):n(Fe^{3+})_{added}$ mole ratio of 3:1 would be expected, that is, one iron(III) ion per three carboxylic acid functions for a very strong interaction. We observed that the actual number of iron(III) ions per carboxylic acid function of the polymer is 0.25 (i.e., the above-mentioned ratio is 4:1). Although it could be ascribed to a weaker interaction in terms of monomeric binding, where the average number of carboxylic acids functions interacting with one iron(III) would be higher than for the above-mentioned scenario, our titration results in the system without additive are in line with the previous study by Scheck et al. [20], where the existence of olation PNCs and the different regimes in the titration curves were established. Further characterization data, i.e., XRD, FTIR, TG-DTA, indicates the formation of Fe(III) (oxy)(hydr)oxide-pGlu composites. The titration data also show that no interaction with the additive occurs after the nucleation point, implying that the additive is actively involved in the nucleation event. This suggests an interaction of the additive with molecular FeOx precursors toward the formation of the solid. Having in mind the hydrolyzing nature of the system, binding of single Fe(III) ions to carboxyl groups up to the saturation level may induce polyelectrolyte iron salt precipitation rather than the observed formation of a composite with 85 wt.% of inorganic phase. The observed $n(COOH):n(Fe^{3+})_{added}$ binding ratio may also be related to the structure and the Fe(III) coordination in the highly-dynamic olation Fe(III) PNCs, namely, some of the carboxyl groups may be sterically inaccessible to Fe(III). After the initial interaction, the Fe(III) olation PNCs formed from the newly added Fe(III) solution probably interact with the already-coordinated Fe(III) PNCs, inhibiting the hydrolysis–polycondensation–nucleation process, which is reflected as a prolonged second stage in the titration curves in the presence of additives, or as a plateau in the $c_{released}(H^{+})/c_{added}(Fe^{3+})$ ratio vs. $c_{added}(Fe^{3+})$ curves, Figures 1d and 2b. Finally, the third stage in the titration curve is characteristic of the post-nucleation stage in the Fe(III) system [20], where no clear effect of the additive is detected.

XRD analysis, Figure 2a, showed that the precipitated solid corresponds to the akagenéite phase, which is usually observed for ambient temperature and low pH values in chloride containing solutions [12]. Remarkably, akagenéite reflections are better defined for the sample prepared with the additive, which is indirectly confirmed by the thermal analysis of the same samples, showing a distinct thermal behavior, Figure 3a. Namely, although both solids after the thermal analysis up to 1000 °C consist of a pure hematite phase, Figure 2a, the corresponding DTA curves apparently indicate that the phase transition is sharply defined for the sample synthesized in the presence of pGlu20, implying a more ordered crystalline structure. The sharp exothermic peak at 357 °C in the DTA curve of the material drawn after titration in the Fe(III)—0.15 g/L pGlu20 sample could originate from the loss of chloride ions from the akagenéite structure and its transformation to hematite [27]. On the other hand, the sample obtained without the additive exhibits broad and undefined exothermic peaks, suggesting a less-ordered structure undergoing thermal crystallization and phase transformation. Although it cannot be undoubtedly confirmed from these experimental data, this transition could be inferred from a small exothermic signal at ~430 °C, implying a lower phase transformation temperature in the case of Fe(III)—0.15 g/L pGlu20 sample. The estimated polymer amount in the composite sample is ~15 wt.%, which makes the material lighter for any possible applications. The improved crystallinity in solids obtained in presence of the polymer is also apparent from the

SEM micrographs of samples derived after titrations in the presence of additives, implying favorable crystallization conditions in the presence of pGlu20.

FTIR analysis, Figure 3b, indicated that the additive structure is well preserved, and no polypeptide denaturation occurred. Although pGlu can be considered fully protonated at pH values between 2 and 3 [28], the characteristic COO- band at 1394 cm^{-1} shifted to 1405 cm^{-1}, implying a more rigid structure, potentially due to the binding of Fe(III). This change should occur during stage I in the titration curve and underlies the initially strong release of protons. Furthermore, there is an apparent change in the amide II spectral region, where broad complex vibration bands disappear and a single-Gaussian band forms. This suggests a change in the hydrogen bonding between polypeptide chain(s), probably due to the changed conformation of the polypeptide in stage II of the titration curve, which is also related to the slight shifting of the amide I band, directly reflecting the change in the backbone conformation.

5. Conclusions

In the present study, we explored the early stages of Fe(III) (oxy)(hydr)oxide formation in the presence of pGlu acid sodium salt with a different number of monomers in the backbone (pGlu20 and pGlu 50). The nucleation behavior was assessed by using an advanced pH-constant titration assay at the pH values of 2.0, 2.5. and 3.0 in combination with additional analyses. The following conclusions can be made:

- The presence of pGlu20/pGlu50 stabilizes the hydrolyzed species, inhibiting phase separation. However, as discussed in detail previously [5], it is challenging to explain this observation from the viewpoint of classical nucleation theory (CNT), which implies that a relatively high concentration of additive is required to alter the nucleation, which would, indeed, rather promote nucleation via heterogeneous pathways because of the dominant interfacial adsorption of the additive on the nuclei's surface.
- The Fe(III) hydrolysis behavior can be divided into three different stages: stage I— characterized by a strong H$^+$ release due to interaction of Fe(III) PNCs with the side-chain carboxylate groups; stage II—stabilization of newly formed Fe(III) PNCs by coordinating with the polypeptide, probably via hydrogen bonding; stage III— uncontrolled hydrolysis and nucleation, where the additive effect is exhausted.
- The change from stage I to stage II in the prenucleation regime occurs at an n(COOH):n(Fe^{3+})$_{added}$ mole ratio of ~4:1 independent of the pH, polymer molecular weight, or concentration.
- The coordination of Fe(III) PNCs and pGlu is accompanied by a change in both hydrogen and electrostatic bonding, yielding a composite of akagénite with 15 wt.% pGlu at pH 3.0 and ambient temperature.
- Detailed analyses (XRD, TG/DTA, SEM) imply that the titrations in the presence of pGlu yielded akagenéite with a higher crystallinity than without the additive, showing that the use of additives is promising for e.g., advanced synthetic strategies of biocompatible lightweight magnetic materials.

Altogether, the effects observed in the presence of pGlu seem incompatible with CNT and should be carefully considered and studied in the frameworks of different nucleation theories. For instance, a possible explanation of our observation lies in the notions of the PNC pathway. Here, the event of phase separation is based on the onset of oxolation within olation PNCs [20]. When olation PNCs are adsorbed on pAsp, the specific distance and environment of partially olated Fe(III) centers might facilitate oxolation [11], while the geometrical situation might be adverse when PNCs are adsorbed on pGlu, due to the additional -CH$_2$_ group in the side chains. This speculative mechanism will have to be studied further in future research. In any case, since corresponding theories should be successful in a holistic manner, studying additive effects on the early stages of mineralization in detail is an alternative avenue toward elucidating mechanisms of nucleation, early growth, and structure formation.

References

1. Baumgartner, J.; Faivre, D. Iron Solubility, Colloids and Their Impact on Iron (oxyhydr)oxide Formation from Solution. *Earth Sci. Rev.* **2015**, *150*, 520–530. [CrossRef]
2. Lowenstam, H.A.; Weiner, S. *On Biomineralization*; Oxford University Press: Oxford, UK, 1989; ISBN 9780195049770.
3. Ciambellotti, S.; Pozzi, C.; Mangani, S.; Turano, P. Iron Biomineral Growth from the Initial Nucleation Seed in L-Ferritin. *Chem. Eur. J.* **2020**, *26*, 5770–5773. [CrossRef]
4. Wang, Z.; Wang, Y.; Wang, Y.; Wei, C.; Deng, Y.; Chen, H.; Shen, J.; Ke, H. Biomineralized Iron Oxide–polydopamine Hybrid Nanodots for Contrast-Enhanced T1-Weighted Magnetic Resonance Imaging and Photothermal Tumor Ablation. *J. Mater. Chem. B* **2021**, *9*, 1781–1786. [CrossRef]
5. Gebauer, D. How Can Additives Control the Early Stages of Mineralisation? *Minerals* **2018**, *8*, 179. [CrossRef]
6. Huang, Z.; Han, F.; Li, M.; Zhou, Z.; Guan, X.; Guo, L. Which Phase of Iron Oxyhydroxides (FeOOH) Is More Competent in Overall Water Splitting as a Photocatalyst, Goethite, Akaganeite or Lepidocrocite? A DFT-Based Investigation. *Comput. Mater. Sci.* **2019**, *169*, 109110. [CrossRef]
7. ThomasArrigo, L.K.; Kaegi, R.; Kretzschmar, R. Ferrihydrite Growth and Transformation in the Presence of Ferrous Iron and Model Organic Ligands. *Environ. Sci. Technol.* **2019**. [CrossRef]
8. Mirabello, G.; Ianiro, A.; Bomans, P.H.H.; Yoda, T.; Arakaki, A.; Friedrich, H.; de With, G.; Sommerdijk, N.A.J.M. Crystallization by Particle Attachment Is a Colloidal Assembly Process. *Nat. Mater.* **2020**, *19*, 391–396. [CrossRef]
9. Zhu, G.; Sushko, M.L.; Loring, J.S.; Legg, B.A.; Song, M.; Soltis, J.A.; Huang, X.; Rosso, K.M.; De Yoreo, J.J. Self-Similar Mesocrystals Form via Interface-Driven Nucleation and Assembly. *Nature* **2021**, *590*, 416–422. [CrossRef]
10. Gebauer, D.; Wolf, S.E. Designing Solid Materials from Their Solute State: A Shift in Paradigms toward a Holistic Approach in Functional Materials Chemistry. *J. Am. Chem. Soc.* **2019**, *141*, 4490–4504. [CrossRef]
11. Scheck, J.; Drechsler, M.; Ma, X.; Stöckl, M.T.; Konsek, J.; Schwaderer, J.B.; Stadler, S.M.; De Yoreo, J.J.; Gebauer, D. Polyaspartic Acid Facilitates Oxolation within iron(III) Oxide Pre-Nucleation Clusters and Drives the Formation of Organic-Inorganic Composites. *J. Chem. Phys.* **2016**, *145*, 211917. [CrossRef]
12. Scheck, J.; Fuhrer, L.M.; Wu, B.; Drechsler, M.; Gebauer, D. Nucleation of Hematite: A Nonclassical Mechanism. *Chem. Eur. J.* **2019**, *25*, 13002–13007. [CrossRef] [PubMed]
13. Thula, T.T.; Svedlund, F.; Rodriguez, D.E.; Podschun, J.; Pendi, L.; Gower, L.B. Mimicking the Nanostructure of Bone: Comparison of Polymeric Process-Directing Agents. *Polymers* **2011**, *3*, 10–35. [CrossRef] [PubMed]
14. Ogunleye, A.; Bhat, A.; Irorere, V.U.; Hill, D.; Williams, C.; Radecka, I. Poly-Γ-Glutamic Acid: Production, Properties and Applications. *Microbiology* **2015**, *161*, 1–17. [CrossRef]
15. Nguyen, Q.T.; Kwak, C.; Lee, W.S.; Kim, J.; Jeong, J.; Sung, M.H.; Yang, J.; Poo, H. Poly-Γ-Glutamic Acid Complexed With Alum Induces Cross-Protective Immunity of Pandemic H1N1 Vaccine. *Front. Immunol.* **2019**, *10*. [CrossRef]
16. Wang, H.; Liu, Y.; Deng, Z.; Han, S. Preparation of Fe3O4/poly(l-Glutamic Acid) Microspheres and Their Adsorption of Cu(II) Ions. *J. Appl. Polym. Sci.* **2016**, *133*. [CrossRef]
17. Yu, Z.; Peng, C.; Luo, Y.; Zhu, J.; Chen, C.; Shen, M.; Shi, X. Poly(γ-Glutamic Acid)-Stabilized Iron Oxide Nanoparticles: Synthesis, Characterization and Applications for MR Imaging of Tumors. *RSC Adv.* **2015**, *5*, 76700–76707. [CrossRef]
18. Mujika, J.I.; Dalla Torre, G.; Formoso, E.; Grande-Aztatzi, R.; Grabowski, S.J.; Exley, C.; Lopez, X. Aluminum's Preferential Binding Site in Proteins: Sidechain of Amino Acids versus Backbone Interactions. *J. Inorg. Biochem.* **2018**, *181*, 111–116. [CrossRef]
19. Lid, S.; Carmona, D.; Maas, M.; Treccani, L.; Colombi Ciacchi, L. Anchoring of Iron Oxyhydroxide Clusters at H and L Ferritin Subunits. *ACS Biomater. Sci. Eng.* **2018**, *4*, 483–490. [CrossRef]
20. Scheck, J.; Wu, B.; Drechsler, M.; Rosenberg, R.; Van Driessche, A.E.S.; Stawski, T.M.; Gebauer, D. The Molecular Mechanism of Iron(III) Oxide Nucleation. *J. Phys. Chem. Lett.* **2016**, *7*, 3123–3130. [CrossRef]

21. Post, J.E.; Buchwald, V.F. Crystal Structure Refinement of Akaganéite. *Am. Mineral.* **1991**, *76*, 272–277.
22. Blake, R.L.; Hessevick, R.E.; Zoltai, T.; Finger, L.W. Refinement of the Hematite Structure. *Am. Mineral.* **1966**, *51*, 123–129.
23. Fulara, A.; Hernik, A.; Nieznańska, H.; Dzwolak, W. Covalent Defects Restrict Supramolecular Self-Assembly of Homopolypeptides: Case Study of β2-Fibrils of Poly-L-Glutamic Acid. *PLoS ONE* **2014**, *9*, e105660. [CrossRef] [PubMed]
24. Sangmi, J.; Jaebum, C.; Daewon, S.; Soo, L.N. Hydrogen Bonding Effects on the Conformational Changes of Polyglutamates Containing Long Flexible Side Chains. *Polymer* **2001**, *42*, 9915–9920.
25. Wang, L.-L.; Chen, J.-T.; Wang, L.-F.; Wu, S.; Zhang, G.; Yu, H.-Q.; Ye, X.; Shi, Q.-S. Conformations and Molecular Interactions of Poly-Γ-Glutamic Acid as a Soluble Microbial Product in Aqueous Solutions. *Sci. Rep.* **2017**, *7*. [CrossRef]
26. Ho, G.-H.; Ho, T.-I.; Hsieh, K.-H.; Su, Y.-C.; Lin, P.-Y.; Yang, J.; Yang, K.-H.; Yang, S.-C. Γ-Polyglutamic Acid Produced by Bacillus Subtilis (Natto): Structural Characteristics, Chemical Properties and Biological Functionalities. *J. Chin. Chem. Soc.* **2006**, *53*, 1363–1384. [CrossRef]
27. Goñi-Elizalde, S.; García-Clavel, M.E. Thermal Behaviour in Air of Iron Oxyhydroxides Obtained from the Method of Homogeneous Precipitation. *Thermochim. Acta* **1988**, *129*, 325–334. [CrossRef]
28. Donten, M.L.; Hamm, P. pH-Jump Induced A-Helix Folding of Poly-L-Glutamic Acid. *Chem. Phys.* **2013**, *422*, 124–130. [CrossRef]